JACS
JOURNAL OF THE AMERICAN CHEMICAL SOCIETY
Article
pubs.acs.org/JACS

Single Molecule Imaging of Oxygenation of Cobalt Octaethylporphyrin at the Solution/Solid Interface: Thermodynamics from Microscopy

Benjamin A. Friesen, Ashish Bhattarai, Ursula Mazur,* and K. W. Hipps*

Department of Chemistry, Washington State University, Pullman, Washington 99164-4630, United States

Supporting Information

ABSTRACT: For the first time, the pressure and temperature dependence of a chemical reaction at the solid/solution interface is studied by scanning tunneling microscopy (STM), and thermodynamic data are derived. In particular, the STM is used to study the reversible binding of O_2 with cobalt(II) octaethylporphyrin (CoOEP) supported on highly oriented pyrolytic graphite (HOPG) at the phenyloctane/CoOEP/HOPG interface. The adsorption is shown to follow the Langmuir isotherm with $P_{1/2}^{298K}$ = 3200 Torr. Over the temperature range of 10−40 °C, it was found that ΔH_P = −68 ± 10 kJ/mol and ΔS_P = −297 ± 30 J/(mol K). The enthalpy and entropy changes are slightly larger than expected based on solution-phase reactions, and possible origins of these differences are discussed. The big surprise here is the presence of any O_2 binding at room temperature, since CoOEP is not expected to bind O_2 in fluid solution. The stability of the bound oxygen is attributed to charge donation from the graphite substrate to the cobalt, thereby stabilizing the polarized Co−O_2 bonding. We report the surface unit cell for CoOEP on HOPG in phenyloctane at 25 °C to be $A = (1.46 \pm 0.1)n$ nm, $B = (1.36 \pm 0.1)m$ nm, and $\alpha = 54 \pm 3°$, where n and m are unknown nonzero non-negative integers.

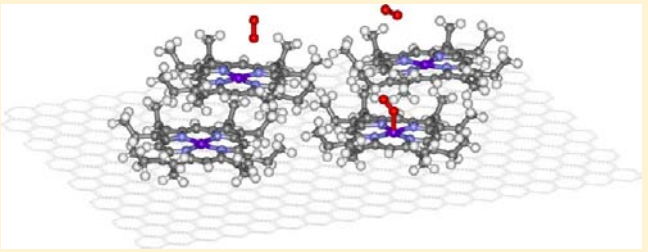

INTRODUCTION

Temperature-dependent studies of surface structures can provide a great wealth of information. They can yield diffusion and reaction rates, activation energies, and thermodynamic quantities, such as entropy and enthalpy of adsorption and/or surface reaction. Because different surface species reach equilibrium at different temperatures and because some surface reactions are kinetically controlled, a study of a given solution−surface pair as a function of temperature can lead to the discovery of new materials and phases. In some cases, the ability to even observe the surface structure is confined to a relatively narrow temperature window, while in others, different structures are observed over a wide temperature range. The ability to observe surface structures as a function of temperature at the solution/solid interface has particular relevance to modern technology, self-assembly, catalysis, friction, film growth, organic electronics, and many other areas.

The study of molecular and even atomic processes at surfaces has been dramatically advanced by the application of the scanning tunneling microscope (STM). There are now about 27 000 papers having "scanning tunneling microscopy" in the title or abstract. If one narrows a SciFinder search to include the "solution interface", the number of citations drops to about 500, still a massive body of literature. There are many tens of papers where samples are separately heated, returned to ambient, and then measured. If one then searches for those papers where molecular level studies are actually performed at the solid/solution interface at a temperature significantly different from room temperature, the total publications drop to a very few,[1−8] with many of these at a single fixed temperature and at least one of the very recent papers inspired by our recent work.[9] A few more papers relate to hot stage designs appropriate for this application (but often focused on atomic force microscopy (AFM) applications).[10−13]

In this work we will use variable temperature STM imaging at the solution/solid interface to determine the thermodynamics of the reversible binding of dioxygen to CoOEP adsorbed on highly oriented pyrolytic graphite (HOPG). Both the variable temperature and single molecule resolution capabilities of the STM are critical for this study. To our knowledge this the first single molecule level study of the temperature dependence of a chemical reaction at the solution/solid interface of any system, not just the dioxygen−CoOEP system. The STM offers unique features including submolecular resolution, sensitivity to electronic structure, ability to function at the solution/solid interface, and variable temperature capability that make it an ideal tool for the study of temperature-dependent surface reactions.

Metalloporphyrins and metallophthalocyanines are a highly versatile family of molecules with widely varying properties and potential applications. Porphyrins and phthalocyanines may serve as components in solar cells,[14] fuel cells,[15] nonlinear optical devices,[16] sensors,[17] and catalysts,[18] serve as sensitizers

Received: May 14, 2012
Published: June 14, 2012

   dx.doi.org/10.1021/ja304431b | J. Am. Chem. Soc. 2012, 134, 14897−14904

in photodynamic tumor therapy,[19] and as components in nanostructured materials.[20,21] The binding of small molecules to metalloporphyrins and metallophthalocyanines is a topic of great interest for a number of reasons. Metalloporphyrins are analogs of hemes, and consequently knowledge of the binding of dioxygen to metalloporphyrins is critical for our understanding of life.[22] Several gas-sensing systems employing metalated porphyrins and phthalocyanines have been reported in the literature. Cobalt phthalocyanine molecules deposited on gold electrodes via organic molecular beam epitaxy show promise as sensors for a variety of species including the Sarin analog dimethyl methylphosphonate.[23,24] The cobalt "picket fence" porphyrin, *meso*-α,α,α,α-tetrakis(*o*-pivalamidophenyl) porphyrinatocobalt(II) imbedded in a polymer matrix functions as an oxygen sensor.[25] Cobalt porphyrins also show promise as electrocatalysts for oxygen reduction.[26−29]

While the binding of dioxygen to cobalt porphyrins is well-known, much of the data reported was gathered at low temperatures (below −20 °C) either in solution[30−37] or in frozen solutions.[38,39] There are relatively few cobalt porphyrins capable of reversibly binding dioxygen at ambient temperatures,[40] most notably cobalt substituted myoglobins[41,42] and the aforementioned cobalt "picket fence" porphyrin *meso*-α,α,α,α-tetrakis(*o*-pivalamidophenyl) porphyinatocobalt(II). This porphyrin binds dioxygen at room temperature in solution[40−47] and in the solid state,[45] but only when a basic axial ligand is present. Kinetic data on the adsorption/desorption of dioxygen to this molecule have been reported at 40 °C, wherein a two-stage adsorption model was proposed.[44]

The enthalpy and entropy changes associated with dioxygen binding to cobalt substituted porphyrins are of interest because cobalt porphyrins serve as model systems for the study of oxygen binding to hemes. Much of the compiled thermodynamic data on cobalt substituted naturally occurring and model porphyrins has been gathered in solution with enthalpy and entropy values ranging from −33 to −56 kJ/mol and −170 to −245 J/(mol K), respectively, when referenced to a 1 Torr standard state for O_2.[30−45] The entropy change associated with dioxygen binding is largely due to the loss of translational and rotational entropy by the bound oxygen as predicted by statistical mechanical calculations.[48]

While it is expected that the affinity for dioxygen binding is strongly dependent on porphyrin species, coordination of the cobalt ion by a fifth ligand can strongly influence equilibrium. Stynes et al. reported on the effects of coordination of basic ligands to the fifth position on dioxygen binding to cobalt(II) protoporphyrin IX dimethyl ester below −30 °C.[30,31] Variation in enthalpy and entropy of oxygenation up to 24% and 15%, respectively, was achieved by changing the fifth ligand. The same study also investigated Hammet relationships among a series of para-substituted pyridines and concluded that oxygen binding is favored by ligands capable of donating electron density to the metal ion to help offset the loss of electron density associated with binding oxygen.[30] Collman et al. have also investigated the effect of coordination of a fifth ligand on oxygenation of cobalt "picket fence" porphyrin at room temperature.[43,45] They showed that cobalt "picket fence" porphyrin binds oxygen to a degree comparable to cobalt substituted myoglobins so long as an imidazole was also bound to the cobalt (in the fifth coordination site). In the absence of a bound imidazole the porphyrin did not bind oxygen at room temperature, thereby underscoring the importance of the fifth coordination site. We also note that Summers and Stolzenberg indicated that ligand binding to the fifth coordination site on cobalt(II) porphyrins relieved strain within the ring system.[49]

Reversible dioxygen binding to cobalt porphyrins and phthalocyanines on surfaces has been reported by groups researching gas sensors[23,24] and gas selective membranes.[25,50,51] Cobalt(II) "picket fence" porphyrin affixed to imidazole and pyridine bases imbedded in membranes is capable of reversibly binding dioxygen with half oxygen saturation pressures ($P_{1/2}$) lower than in solution or as a crystal. The $P_{1/2}$ of Co "picket fence" porphyrin in toluene with 1-methylimidazol coordinated at the fifth site is 140 Torr at 25 °C,[45] while the same porphyrin bound to an imidazol-terminated polymer reaches half saturation at 74 Torr at 25 °C;[51] close to the $P_{1/2}$ of crystalline porphin/1-methylimidazol (61 Torr) at 25 °C.[45] The enthalpy of oxygenation for the porphyrin/imidazol pair increases in the order of solution (−51.0 kJ/mol)[45] to solid state (−55.6 kJ/mol)[45] to the membrane-bound porphyrin (−58.6 kJ/mol).[51] The entropy change, referenced to a 1 Torr standard state, upon oxygen binding is less dramatic in this case. The values increase from −214 J/(mol K in toluene solution[43] to −223 J/(mol K) in the solid state.[45] Summers et al. state that the entropy change for the membrane[51] is similar to that in solution.

The subject of this study, CoOEP, is a known electrocatalyst for the reduction of oxygen[27,52] and shows promise as a gas sensor due to its capability to bind volatile organic molecules.[53,54] Interestingly, Yamazaki et al. have demonstrated that substrate choice can impact the onset potential of oxygen reduction by cobalt porphyrins by almost 200 mV.[27] CoOEP reversibly binds carbon monoxide at ambient temperatures[55] but will bind dioxygen only at low temperatures (<−90 °C).[56−59] The dioxygen complex was investigated by Raman, infrared, Mössbauer, and electron spin resonance spectroscopies. In all but one of the studies an axial base was used. In that latter study, the dioxygen adduct was reported to form in argon matrices at 15 K without the addition of a fifth ligand.[56] No thermodynamic data for adduct formation were reported.

EXPERIMENTAL SECTION

2,3,7,8,12,13,17,18-Octaethyl-21*H*,23*H*-porphine cobalt(II) [CoOEP] was purchased from Aldrich. Reagent grade chloroform was purchased from J.T. Baker. Phenyloctane (99%) was purchased from Alfa Aesar. All reagents were used without further purification. The 1 cm^2 highly ordered pyrolytic graphite (HOPG) substrates (grade 2) were purchased from SPI supplies (West Chester, Pa., no. 436HP-AB, lot no. 1160321). STM images were recorded using a Molecular Imaging (now Agilent) Pico 5 STM equipped with a 1 μm^2 head and an environmental chamber. STM tips were made by cutting or electrochemically etching $Pt_{0.8}Ir_{0.2}$ wire (California Fine Wire Company Grover Beach, Ca.). Images were typically obtained at a sample potential of −0.5 V and a tunneling current of 20 pA. Scan rates typically were 4.7 lines/sec, giving a total image time of 2.0 min. The temperature of the sample was controlled by either a variable-temperature hot stage or a 1X Peltier stage using a Lakeshore 330 autotuning temperature controller. Temperature was monitored with a calibrated Pt resistance thermometer. Stock solutions of CoOEP were prepared by dissolving sufficient solid CoOEP in chloroform to make a solution of concentration 200 μM. This solution was subsequently diluted to about 9 μM in chloroform. STM samples were prepared by dropping a 25 μL aliquot of the 9 μM CoOEP solution on a freshly peeled 1 cm^2 HOPG substrate and allowing the solvent to evaporate. The dried surface was then covered with phenyloctane, and the resulting sample was then placed on the heating stage and transferred into the controlled atmosphere chamber of the STM. It should be

noted that samples prepared from pure chloroform in this way showed no structured adsorbates and appeared to be clean graphite. This is worth noting since the weight/weight ppm of CoOEP in chloroform is 3.6 ppm, and the solid residue specification for the reagent used is <1 ppm.

The partial pressure of oxygen over the sample was controlled by flowing mixtures of argon and oxygen gas into the STM chamber. Oxygen and argon flows were controlled by individual flow meters (model 7200 King Instrument Company, Garden Grove, CA). Partial pressures were determined as the ratio of $O_2/(O_2 + Ar)$ times the measured barometric pressure. The gases used had the following purity: 99.995% Ar with water <5 ppm, O_2 <5 ppm, and THC <2 ppm; 99.995% O_2 with water <5 ppm and THC <2 ppm; and N_2 with water <5 ppm, O_2 < 5 ppm, and THC < 2 ppm.

The sample (in the STM chamber) was first annealed at 100 °C for 10 min under pure argon flowing at 2.5 standard cubic feet per hour (scfh). Prior to recording images the samples were allowed to equilibrate for at least three hours at the oxygen partial pressure and temperature of interest. All images were recorded while scanning in a drop of phenyloctane. All STM images were background subtracted using SPIP[60] image processing software and drift corrected using a linear drift correction algorithm.[61,62]

Solution-phase oxygen binding studies were carried out using a Perkin-Elmer model 330 spectrophotometer with 1 cm path length cuvettes. All samples for solution-phase oxygen-binding experiments were prepared in reagent grade toluene degassed by boiling for 45 min followed by cooling to room temperature. The toluene was continuously purged with nitrogen during the degassing process. A 1 μM solution of CoOEP prepared using the degassed toluene was split into two equal samples. Oxygen gas was bubbled through one of the samples for 24 h. After oxygen exposure, the CoOEP solution was analyzed by UV−vis spectroscopy. A duplicate control sample was exposed to nitrogen for 24 h and subsequently analyzed by UV−vis spectroscopy. Appropriate blanks were prepared by exposing toluene to either oxygen or nitrogen gas.

RESULTS AND DISCUSSION

Figure 1 is the structure of CoOEP in the all-up or crown configuration of the ethyl groups. This is the known orientation

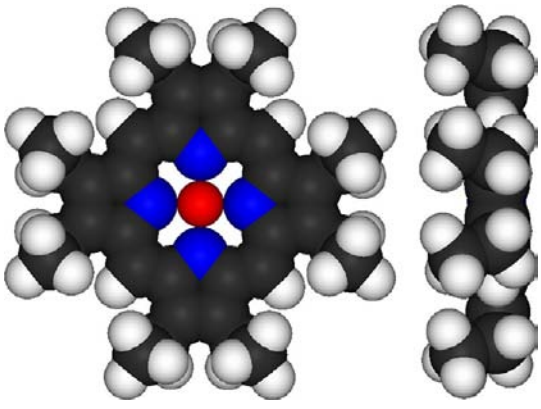

Figure 1. Model of "crown" configuration of CoOEP derived from DFT calculation (top and side views). Black atoms are carbon, white are hydrogen, blue are nitrogen, and red are cobalt. The Gaussian03 com file for this structure is available as Supporting Information.

of the ethyl groups for NiOEP adsorbed on Au(111)[63] and is the presumed configuration for CoOEP on HOPG. The space filling models used later are based on optimization of this configuration by DFT calculations using the B3LYP functional and the 6-311++G(d,p) basis. The actual optimized structure is provided as a Gaussian03 com file in the Supporting Information. We also used the B3LYP functional and a much larger basis 6-311++G(d,p) on C, N, and H and 6-311+G(3df) on O and Co to estimate the structure of the O_2−CoOEP adduct.

To confirm previous results that pure CoOEP will not bind O_2 in solution at room temperature, we measured UV−vis spectra of O_2 and N_2 saturated solutions in toluene after 24 h of exposure. Figure 2 demonstrates that there is no change in either the Soret or Q bands, indicating that no adduct forms under these conditions.

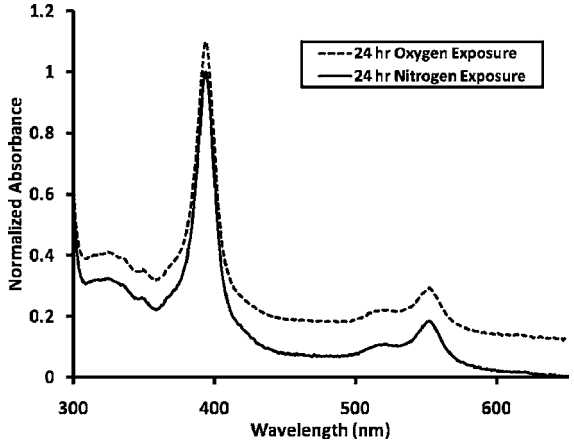

Figure 2. UV−vis spectrum of CoOEP in toluene solution after 24 h exposure to O_2 and to N_2, respectively. The oxygenated solution data is manually offset upward to aid comparison.

Figure 3 presents a representative image obtained from the HOPG supported CoOEP surface covered in phenyloctane and at equilibrium with a pure O_2 atmosphere at 25 °C. There are clearly three types of sites in the image. Those enclosed by squares are very deep and are vacancies in the monolayer. Those enclosed by circles have apparent heights about half that of the other molecular features. By performing the same measurements on monolayers annealed at 100 °C in pure argon, it is clear that the bright (high) features are simply CoOEP. This is consistent with a number of previous studies wherein it was demonstrated that tunneling through the half-filled d_z^2 orbital produces the bright molecular center.[64−66]

The components of a mixed monolayer of cobalt(II) hexadecafluoro-29*H*,23*H*-phthalocyanine and nickel(II) tetraphenyl 21*H*,23*H*-porphine can easily be differentiated in STM images by the bright half-filled d_z^2 orbital in the cobalt species as opposed to the darker Ni atoms.[65] The STM is also capable of detecting axial groups attached to porphyrins and phthalocyanines. Vanadyl phthalocyanine centers appear dark in STM images due to oxygen's lack of states near the Fermi level.[66,67] The striking difference in the STM contrast of bright cobalt with dark vanadyl octaethyl porphyrins adsorbed on graphite was also well demonstrated by Miyake et al.[68] It is the STM's ability to differentiate the bright half-filled d_z^2 orbital in cobalt coupled with the expected attenuated signal in the oxygenated species which allow oxygenated and deoxygenated cobalt porphyrins to be distinguished and consequently thermodynamic data to be gathered on a molecule by molecule basis.

In order to verify our interpretation of the bright and dark features, STM images at varying equilibrium partial pressures of O_2 were measured and analyzed. Defining the surface coverage of dark molecules, Θ, as the number of dark molecules divided

dx.doi.org/10.1021/ja304431b | J. Am. Chem. Soc. 2012, 134, 14897−14904

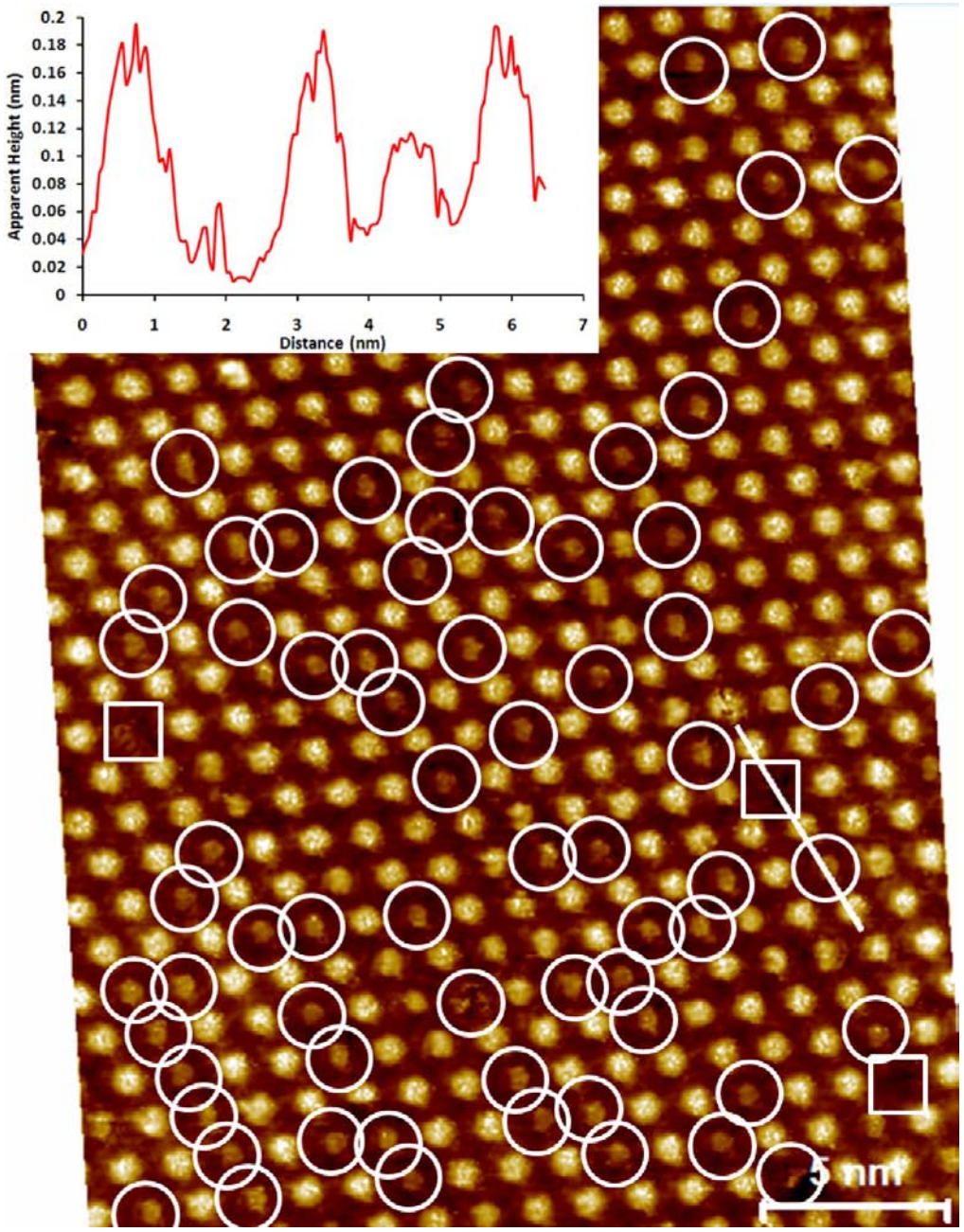

Figure 3. Drift-corrected constant current STM image of the phenyloctane/CoOEP/HOPG interface under conditions of O_2 saturation at 25C. STM data were acquired at −0.5 V and 20 pA set point. Note that the molecules enclosed in circles are considerably dimer than others, and the squares identify vacancies in the monolayer. The inset is a cross section emphasizing the differences between the bright and the dim molecules.

by the total number of surface molecules, one would expect the quantity $\Theta/(1-\Theta)$ to be proportional to the partial pressure of O_2 provided that the dark molecules were sites of O_2 adsorption, and the Langmuir isotherm is followed. Figure 4 clearly shows that this is the case. Thus, the equilibrium constant for the O_2 adsorption process, K_P, is given by

$$K_P = \frac{\Theta}{(1-\Theta)(P/P^0)}$$

where following the convention in solution-phase studies we have taken the standard state to be P^0 = 1 Torr. Alternatively, one might relate the equilibrium constant to the molal concentration of O_2 in solution, K_c,

$$K_c = \frac{\Theta}{(1-\Theta)(c/c^0)}$$

where c^0 is the hypothetical ideal state of 1 *m* of O_2 in solution. Using $\Delta G_{P,c} = -RT\ln(K_{P,c})$, one can determine the free energy change for the

$$O_2 + \text{CoOEP/HOPG} = O_2\text{–CoOEP/HOPG}$$

system in the appropriate standard state. $\Delta S_{P,c} = -(\partial G/\partial T)_{P,c}$ for the appropriate standard state, and $\Delta H_{P,c} = \Delta G_{P,c} + T\Delta S_{P,c}$, thereby allowing all the thermodynamic functions to be obtained from a series of STM measurements at various temperatures. The two sets of thermodynamic quantities (at fixed *c* or fixed *P*) are connected by the temperature-dependent

dx.doi.org/10.1021/ja304431b | *J. Am. Chem. Soc.* 2012, 134, 14897−14904

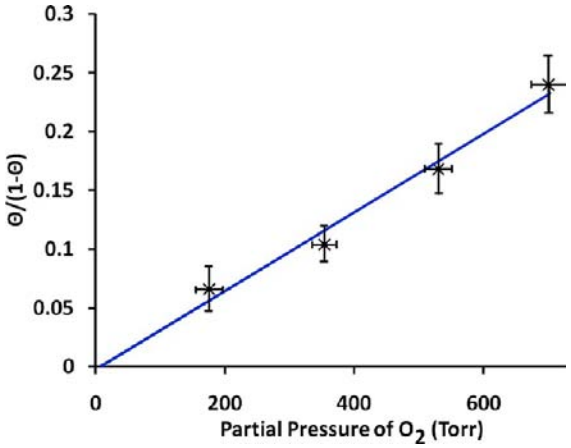

Figure 4. Langmuir plot of relative surface coverage of dark molecules as a function of O_2 partial pressure at 25 °C.

Henry's law constant. The thermodynamics that are derived from their temperature dependences differ by the heat and entropy of solution of O_2 in phenyloctane.

Before proceeding with the thermodynamic analysis, it is important to ascertain the reliability in the values of Θ obtained. Thus, the Θ value used for each temperature was the average of a large number of separate measurements of STM images. The standard deviations in these measurements were used to determine the vertical error bars (±1 SD) in each figure. To ensure that the system had come to equilibrium, these were measured after a considerable wait and over a long period of time. A representative set of such measurements is displayed in Figure 5. The data in Figure 5 were collected after

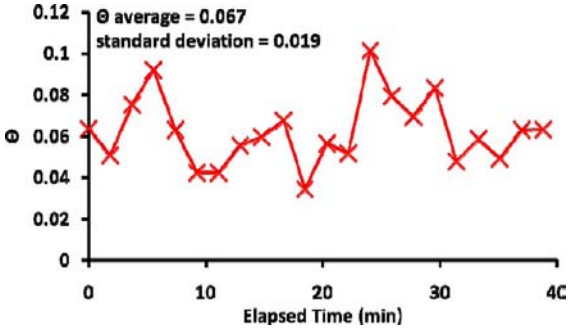

Figure 5. Variation in measurements of Θ with time (after a 4 h wait) for $P(O_2)$= 176 Torr and 25 °C.

the system had been allowed to come to equilibrium for 4 h. We note that each image analyzed contained about N = 250 molecules. However, at 25 °C and 176 Torr, the average coverage of oxygenated species is only about 7% of the 250 molecules or 18 oxygenated molecules, resulting in an expected statistical fluctuation of $(1/N)^{1/2}$, or ±23%, which is of the order observed in Figure 5.

In order to determine $K(T)$, values of Θ were extracted from STM images acquired at various temperatures and 100% O_2 saturation and 704 Torr. Figure 6 shows three of the many images analyzed as a function of temperature between 10 and 40 °C. Data were not acquired above 40 °C because the number of oxygenated sites had become too few to have statistical significance. It should be noted that the appearance of the bright center varied with tip quality. For a very sharp tip the bright region was small and intense. For a dull tip, most of the molecule appeared bright. In all cases it was easy to distinguish the dim and bright molecules within a given image. It should be further noted that the "dim" molecules can also be distinguished from vacancies in the monolayer. The central image in Figure 6 shows a cross section through three bright molecules, one dim one and a true vacancy (surrounded by a square).

Using average values and standard deviations for Θ determined in the manner above for 100% O_2 atmosphere (P = 704 Torr) at various temperatures, one can determine values of ΔG_P as a function of temperature, as shown in Figure 7. From the slope of these data with temperature, ΔS may be determined. With these, one may calculate ΔH. Thus, one arrives at $\Delta H_P = -68 \pm 10$ kJ/mol and $\Delta S_P = -297 \pm 30$ J/(mol K).

One may also report thermodynamic values referenced to the hypothetical ideal 1 m (of O_2) state. These are denoted by subscript c. Thus, $\Delta G_P = \Delta G_c + \Delta G_H$, $\Delta H_P = \Delta H_c + \Delta H_H$, and $\Delta S_P = \Delta S_c + \Delta S_H$, where the H subscript refers to the change in thermodynamic quantity with respect to formation of the solution from the ideal gas phase (Henry's law). While the Henry's law constant for phenyloctane is not available as a function of temperature, values for two closely related compounds, toluene and octane, are available.[69,70] Thus, one can estimate ΔH_c and ΔS_c based on the range seen for these solvents. ΔH_c(toluene) = −72 ± 10 kJ/mol, and ΔS_c(toluene) = −211 ± 30 J/(mole K), while ΔH_c(octane) = −68 ± 10 kJ/mol, and ΔS_c(octane)= −204 ± 30 J/(mole K). Because ΔH for solvation of O_2 is small in these solvents, there is no significant effect on ΔH_c, and we can reasonably say that ΔH_c (phenyloctane) = −70 ± 15 kJ/mol. While ΔS for solvation of O_2 is large, it is essentially the same for both these solvents. Thus, it is reasonable to estimate ΔS_c (phenyloctane) = −208 ± 24 J/(mole K). Because it is common to do so in the solution-phase oxygen-binding literature, we used our data to determine the $P_{1/2}$(298 K), the O_2 partial pressure at which half the sites on the CoOEP/HOPG surface would be occupied by O_2. We found that $P_{1/2}$(298 K) = 3200 Torr, or about four atmospheres of oxygen.

These results are extremely surprising. Qualitatively, the reversible binding of O_2 by CoOEP/HOPG is a surprise. Based on solution-phase studies, one does not expect to see reversible binding of O_2 by CoOEP at room temperature. Even the addition of pyridine bases to the fifth coordination site is not sufficient to produce O_2 binding at 298 K. Nevertheless, the HOPG-bound CoOEP is binding oxygen and doing so with sufficient residence time to allow observation by STM imaging. Extending arguments derived from solution-phase studies, such as those of Collman[48,45] and Stynes,[30,31] it appears that the HOPG surface is strongly donating electrons to the cobalt center, thereby stabilizing the polarized Co−O_2 complex. Quantitatively, the results provide a mixed message. The value of ΔH_P (−68 kJ/mol) is more negative than the larger values reported for cobalt complexes in solution (about −60 kJ/mol) but is consistent with the unusually large binding and long residence time observed for O_2 on CoOEP/HOPG. The value of ΔS_P [−297 J/(mol K)] is more negative than previous reports for solution and solid-state binding by cobalt complexes [about −230 J/(mol K)] and also slightly larger than the negative of the absolute entropy for the O_2 molecule at 1 Torr and 298 K calculated from statistical mechanics (−268 J/mol K).

dx.doi.org/10.1021/ja304431b | J. Am. Chem. Soc. 2012, 134, 14897−14904

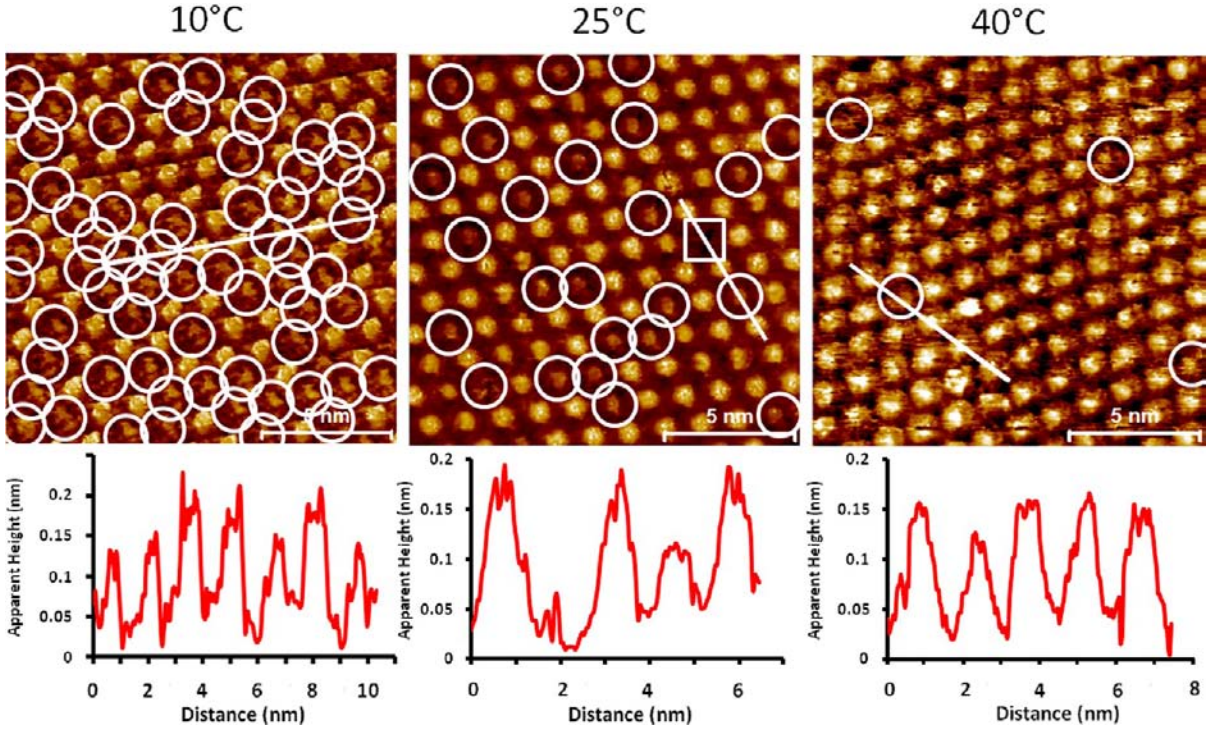

Figure 6. Representative constant current STM data acquired at 10 °C (left), 25 °C (middle), and 40 °C (right).

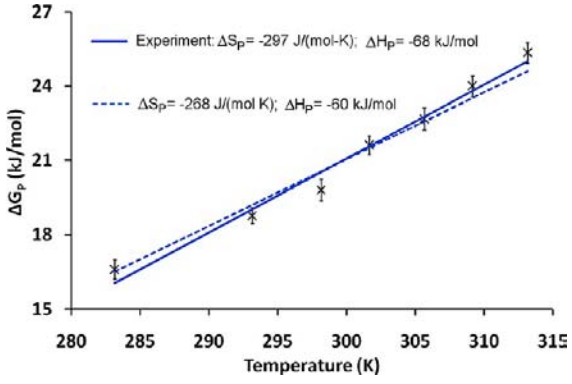

Figure 7. ΔG_P as a function of temperature. The slope of the solid blue line is the measured ΔS_P, the entropy change relative to the 1 Torr standard state. For reference, a dotted line is shown with slope equal to the ΔS_P based solely upon the entropy of O_2 at 298 K.

Since ΔS_P is based on the slope, it is less accurate than the change in free energy, and the possibility of numerical error must be addressed. To that end, a line of slope −268 J/(mol K) and ΔH_P = −60 kJ/mol is drawn over the actual free energy data in Figure 7. In order for the correct value of the slope to be −268 J/(mol K), it would require only a slight deviation from the least-squares best fit line and would fall within 1 SD of all but one of the measured values. We consider this very good agreement with the expectations derived from statistical mechanics. We also note that the associated ΔH_P is close to values determined for other room temperature oxygen binders. One might argue that not all the rotational entropy of O_2 is lost because there is probably some hindered rotational motion over the four-fold porphyrin pocket. Where then might this additional entropy be lost? A possibility is that the O_2 binding is inducing some additional order in the solvent, the porphyrin ring, or both.

A possibility worth considering is that there is more than one type of adsorption/desorption process and that the second (or more) process is occurring too fast to be followed by STM. While we cannot eliminate this from consideration, the implication is that there is significantly more bound O_2 than we have observed. Since the amount seen with the STM is already higher than expected, the existence of an unrelated fast mechanism appears less likely.

The large binding of O_2 on CoOEP adsorbed on HOPG is not so surprising when viewed in the context of recent ultrahigh vacuum (UHV) studies of metal porphyrins on surfaces. It was shown in the 1980s that cobalt(II) tetraphenylporphyrin (CoTPP) supported on TiO_2 powder catalyzes the reduction of NO and NO_2 in the presence of CO and H_2 with high efficiency despite the fact that neither the free-standing CoTPP nor the TiO_2 powder is reactive on its own.[71] This was explained by saying that electronic structure of the Co ion was modified by partial electron transfer from the TiO_2 support. Recently there have been a number of UPS, XPS, and STS studies suggesting that metalloporphyrins couple electronically to metal surfaces.[72−74] A very recent systematic study of metal tetraphenylporphyrins on silver clearly shows the surface behaving as a fifth coordination site in a "surface trans effect".[75] Thus, there is precedent in the literature for a substrate to act as an electron-donating fifth ligand on the metal ion of an adsorbed metal porphyrin.

A different facet of this study of interest to surface science is the structure of the monolayer of CoOEP. Figure 8 shows a portion of a drift corrected STM image and one possible set of molecular orientations that generate the observed surface pattern. Unlike the UHV study of NiOEP, we could not resolve the ethyl groups.[63] Thus, we were forced to rely on simple model building to arrive at a possible structure. Correctly scaled models (based on the DFT calculated geometry) were placed over the image in a manner that appeared to minimize overlap

dx.doi.org/10.1021/ja304431b | J. Am. Chem. Soc. 2012, 134, 14897−14904

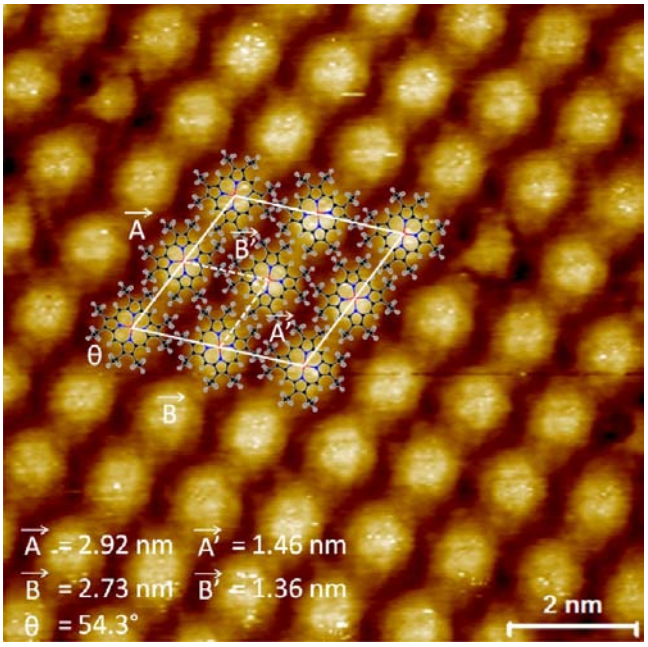

Figure 8. Possible unit cell parameters for CoOEP/HOPG in phenyloctane at 25 °C. A = (1.46 ± 0.1 nm)n, B = (1.36 ± 0.1 nm)m, and α = 54.3 ± 4°.

of ethyl groups. As shown in Figure 8, this resulted in a body centered unit cell at 25 °C having A = 2.92 ± 0.15 nm, B = 2.73 ± 0.15 nm, and θ = 54 ± 3°. This cell results from a relative rotation of 18° between molecules along the A direction. If one ignores the attempt to optimize packing and simply uses the molecular pattern, a smaller lattice having only one molecule per unit cell results with A' = 1.41 ± 0.1 nm, B' = 1.36 ± 0.1 nm, and α = 54 ± 4°. These values can be compared to those reported for CoOEP/HOPG deposited from 1-tetradecene by Miyake et al.[68] They gave A' = 1.48 ± 0.1 and B' = 1.42 ± 0.1, in reasonable agreement with the low-resolution pattern. In the absence of high-resolution images, any integer multiple (nA', mB') of A' and B' might be the actual surface structure.

CONCLUSIONS

It has been demonstrated that variable-temperature STM can be used to determine adsorption isotherms and thermodynamic data for processes occurring at the solid/solution interface. We have shown that the solid support (in this case HOPG) can act in a manner similar to an electron-donating ligand bound to the fifth coordination site on the cobalt ion of CoOEP, thereby greatly increasing the compound's affinity for oxygen. The free energy, enthalpy, and entropy changes associated with the O_2 binding process are determined for the first time and found to be qualitatively correct but larger than previously observed for purely solution-phase reactions. While this difference may be due to surface and solvent reorganization, certain determination will require extending the temperature range of these measurements to lower temperatures, which we plan to do. Another obvious extension of this work is the measurement of the binding process on substrates having different chemical properties and work functions. This is also underway.

This work presents a novel approach for obtaining thermodynamic quantities and a better understanding of the fundamental chemistry of reactions of dioxygen with metal–organic complexes at the single-molecule level in solution environments. The experimental conditions used here allow one to mimic the chemical events of biological oxidation and in situ heterogeneous catalysis. Using a metal substrate as the fifth ligand allows for the formation of transition metal–dioxygen binding complexes, where the bound dioxygen is held in a sterically protected site, which in principle precludes dimerization and other unwanted reactions that may occur in a solution phase.

ASSOCIATED CONTENT

Supporting Information

Gaussian com file for the optimized geometry shown in Figure 1. This material is available free of charge via the Internet at http://pubs.acs.org.

AUTHOR INFORMATION

Corresponding Author

umazur@wsu.edu; hipps@wsu.edu

Notes

The authors declare no competing financial interest.

ACKNOWLEDGMENTS

This material is based upon work supported by the National Science Foundation under grants CHE-1152951, CHE-1112156, and CHE-1058435.

REFERENCES

(1) Askadskaya, I.; Rabe, J. P. *Phys. Rev. Let.* **1992**, *69*, 1395–1398.
(2) Walch, H.; Maier, A.; Heckl, W.; Lackinger, M. *J. Phys. Chem. C* **2009**, *113*, 1014–1019.
(3) Ramachandran, G. K.; Hopson, T. J.; Rawlett, A. M.; Nagahara, L. A.; Primak, A.; Lindsay, S. M. *Science* **2003**, *300*, 1413–1416.
(4) Marie, C.; Silly, F.; Tortech, L.; Mullen, K.; Fichou, D. *ACS Nano* **2010**, *4*, 1288–1292.
(5) Giesen, M.; Baier, S. *J. Phys.: Condens. Matter* **2001**, *13*, 5009–5026.
(6) MacLeod, J.; Rosei, F. *Aust. J. Chem.* **2011**, *64*, 1297–1298.
(7) Solid–Liquid Interfaces. *Topics in Applied Physics*; Dretschkow, T., Wandlowski, T., Wandelt, K., Thurgate, S., Eds.; Springer-Verlag: Berlin Heidelberg, 2003; Vol. *85*, pp 259–324.
(8) English, W.; Hipps, K. W. *J. Phys. Chem. C* **2008**, *112*, 2026–2031.
(9) Gutzler, R.; Sirtl, T.; Dienstmaier, J. F.; Mahata, K.; Heckl, W. M.; Schmittel, M.; Lackinger, M. *J. Am. Chem. Soc.* **2010**, *132*, 5084–5090.
(10) Lindsay, S. M. CODEN: USXXAM US. U.S. Patent 5654546 A 19970805, 1997.
(11) Oulevey, F.; Gremaud, G.; Kulik, A. J.; Guisolan, B. *Rev. Sci. Instrum.* **1999**, *70* (3), 1889–1890.
(12) Trawick, M. L.; Angelescu, D. E.; Chaikin, P. M.; Valenti, M. J.; Register, R. A. *Rev. Sci. Instrum.* **2003**, *74* (3, Pt. 1), 1390–1392.
(13) Sattin, B.. D.; Goh, M. C. *Rev. Sci. Instrum.* **2004**, *75* (11), 4778–4780.
(14) Campbell, W. M.; Jolley, K. W.; Wagner, P.; Wagner, K.; Walsh, P. J.; Gordon, K. C.; Schmidt-Mende, L.; Nazeerudding, M. K.; Wang, Q.; Ratzel, M.; Officer, D. L. *J. Phys. Chem. Lett.* **2007**, *111*, 11760–11762.
(15) Shi, Z.; Zhang, J. *J. Phys. Chem. C* **2007**, *111*, 7084–7090.
(16) Yao, C.; Yan, L.; Guan, L.; Liu, C.; Song, P.; Su, Z. *Dalton Trans.* **2010**, *39*, 7645–7649.
(17) Thyagariajan, S.; Leiding, T.; Arskold, S. P.; Cheprakov, A. V.; Vinogradov, S. A. *Inorg. Chem.* **2010**, *49*, 9909–9920.
(18) Riberio, S. M.; Serra, A. C.; Rocha Gonsalves, A.M.d'A. *J. Mol. Catal. A* **2010**, *326*, 121–127.
(19) Verma, A.; Facchina, S. L.; Hirsch, D. J.; Song, S.; Dillahey, L. F.; Williams, J. R.; Snyder, S. H. *Mol. Med.* **1998**, *4*, 40–45.

(20) Hu, J. S.; Ji, H. X.; Wan, L. *J. Phys. Chem. C* **2009**, *113*, 16259−16265.
(21) Friesen, B. A.; Wiggins, B.; McHale, J. L.; Mazur, U.; Hipps, K. W. *J. Am. Chem. Soc.* **2010**, *132*, 8554−8556.
(22) Momenteau, M.; Reed, C. A. *Chem. Rev.* **1994**, *94*, 659−698.
(23) Bohrer, F. I.; Sharoni, A.; Colesniuc, C.; Park, J.; Schuller, I. K.; Cummel, A. C.; Trogler, W. C. *J. Am. Chem. Soc.* **2007**, *129*, 5640−5646.
(24) Bohrer, F. I.; Colesniuc, C. N.; Park, J.; Ruidiaz, M. E.; Schuller, I. K.; Kummel, A. C.; Trogler, W. C. *J. Am. Chem. Soc.* **2009**, *131*, 478−485.
(25) Hyakutake, T.; Okura, I.; Asai, K.; Nishide, H. *J. Mater. Chem.* **2008**, *18*, 917−922.
(26) Su, B.; Hatay, I.; Trojanek, A.; Samec, Z.; Khoury, T.; Gros, C. P.; Barbe, J. M.; Daina, A.; Carrupt, P. A.; Girault, H. H. *J. Am. Chem. Soc.* **2010**, *132*, 2655−2662.
(27) Yamazaki, S.; Yamada, Y.; Ioroi, T.; Fujiwara, N.; Siroma, Z.; Yasuda, K.; Miyazaki, Y. *J. Electroanal. Chem.* **2005**, *576*, 253−259.
(28) Steiger, B.; Anson, F. C. *Inorg. Chem.* **2000**, *39*, 4579−4585.
(29) Yu, H. .Z.; Baskin, J. S.; Steiger, B.; Anson, F. C.; Zewali, A. H. *J. Am. Chem. Soc.* **1999**, *121*, 484−485.
(30) Stynes, D. V.; Stynes, H. C.; James, B. R.; Ibers, J. A. *J. Am. Chem. Soc.* **1973**, *95*, 1796−1801.
(31) Stynes, H. C.; Ibers, J. A. *J. Am. Chem. Soc.* **1972**, *94*, 5125−5127.
(32) Beugelsdijk, T. J.; Drago, R. S. *J. Am. Chem. Soc.* **1975**, *97*, 6466−6470.
(33) Linard, J. E.; Ellis, P. E., Jr.; Budge, J. R.; Jones, R. D.; Basolo, F. *J. Am. Chem. Soc.* **1980**, *102*, 1896−1904.
(34) Walker, F. A. *J. Am. Chem. Soc.* **1973**, *95*, 1154−1159.
(35) Yamamoto, H.; Takayanagi, T.; Kwan, T.; Yonetani, T. *Bioinorg. Chem.* **1977**, *7*, 189−201.
(36) Stynes, H. C.; Ibers, J. A. *J. Am. Chem. Soc.* **1972**, *94*, 1559−15562.
(37) Uruma, K.; Tsuge, K.; Sasaki, Y.; Imamura, T. *Chem. Lett.* **2005**, *34*, 474−475.
(38) Nakayama, S; Tani, F.; Matsu-ura, M.; Naruta, Y. *Chem. Lett.* **2002**, 496−497.
(39) Walker, F. A. *J. Amer. Chem. Soc.* **1970**, *92*, 4235−4244.
(40) Steiger, B.; Baskin, J. S.; Anson, F. C.; Zewail, A. H. *Angew. Chem., Int. Ed.* **2000**, *39*, 257−260.
(41) Wang, M. Y. R.; Hoffman, B. M.; Shire, S. J.; Gurd, F. R. N. *J. Am. Chem. Soc.* **1979**, *101*, 7394−7397.
(42) Spilburg, C. A.; Hoffman, B. M.; Petering, D. H. *J. Bio. Chem.* **1972**, *247*, 4219−4223.
(43) Collman, J. P.; Brauman, J. I.; Doxsee, K. M.; Halbert, T. R.; Suslick, K. S. *Proc. Natl. Acad. Sci. U.S.A.* **1978**, *75*, 564−568.
(44) Zou, S.; Baskin, J. S.; Zewail, A. H. *Proc. Natl. Acad. Sci. U.S.A.* **2002**, *99*, 9625−9630.
(45) Collman, J. P.; Brauman, J. I.; Doxsee, K. M.; Halbert, T. R.; Hayes, S. E.; Suslick, K. S. *J. Am. Chem. Soc.* **1978**, *100*, 2761−2766.
(46) Li, J.; Oliver, A. G.; Ferraudi, G.; Lappin, A. G.; Scheidt, W. R. *Inorg. Chem.* **2010**, *49*, 2398−2406.
(47) Valiotti, A. B.; Abakumova, R. A. *Rus. J. Appl. Chem.* **2007**, *77*, 1623−1626.
(48) Collman, J. P.; Brauman, J. I.; Suslick, K. S. *J. Am. Chem. Soc.* **1975**, *97*, 7185−7186.
(49) Summers, J. S.; Stolzenberg, A. M. *J. Am. Chem. Soc.* **1993**, *15*, 10559−10567.
(50) Nishide, H.; Suzuki, T.; Nakagawa, R.; Tsuchida, E. *J. Am. Chem. Soc.* **1994**, *116*, 4503−4504.
(51) Suzuki, Y.; Nishide, H.; Tsuchida, E. *Macromolecules* **2000**, *33*, 2530−2534.
(52) Song, E.; Shi, C.; Anson, F. C. *Langmuir* **1998**, *14*, 4315−4321.
(53) Capan, I.; Tarimci, C.; Capan, R. *Sens. Actuators, B* **2010**, *144*, 126−130.
(54) Akrajas, M.; Salleh, M.; Yahaya, M. *Sens. Actuators, B* **2002**, *85*, 191−196.
(55) Schmidt, E.; Zhang, H.; Chang, C. K.; Babcock, G. T.; Oertling., W. A. *J. Am. Chem. Soc.* **1996**, *118*, 2954−2961.
(56) Urban, M. W.; Nakamoto, K. *Inorg. Chim. Acta* **1982**, *61*, 77−81.
(57) Baumgarten, M.; Winscom, C. J.; Lubitz, W. *Appl. Magn. Reson.* **2001**, *20*, 1−36.
(58) Sakai, H.; Maeda, Y.; Ogoshi, H.; Sugimoto, H.; Yoshida, Z. *Chem. Lett.* **1978**, 353−356.
(59) Bajdor, K.; Kincaid, J. R.; Nakamoto, K. *J. Am. Chem. Soc.* **1984**, *106*, 7741−7747.
(60) *SPIP*; Image Metrology: Hørsholm, Denmark.
(61) Tong, W.; Xue, Y.; Zimmt, M. B. *J. Phys. Chem. C* **2010**, *114*, 20783−20792.
(62) Tong, W. Controlling Self-Assembled Monolayer Morphology with Dipolar Interactions: Preparation, STM Image Analysis and Simulations of 1,5-(Disubstituted)-Anthracene Monolayers. Ph.D. Thesis, Brown University, Providence, RI, 2010.
(63) Scudiero, L.; Barlow, D. E.; Hipps, K. W. *J. Phys. Chem. B* **2002**, *106*, 996−1003.
(64) Scudiero, L.; Barlow, D. E.; Hipps, K. W. *J. Phys. Chem. B* **2000**, *104*, 11899−11905.
(65) Hipps, K. W.; Scudiero, L.; Barlow, D. E.; Cooke, M. P., Jr. *J. Am. Chem. Soc.* **2002**, *124*, 2126−2127.
(66) Barlow, D. E.; Hipps, K. W. *J. Phys. Chem. B* **2000**, *104*, 5993−6000.
(67) Mazur, U.; Hipps, K. W.; Reichers, S. L. *J. Phys. Chem. C* **2008**, *112*, 20347−20356.
(68) Miyake, Y.; Tanaka, H.; Ogawa, T. *Colloids Surf., A* **2008**, *313−314*, 230−233.
(69) Li, A.; Tang, S.; Tan, P.; Liu, C.; Liang, B. *J. Chem. Eng. Data* **2007**, *52*, 2339−2344.
(70) Battino, R.; Rettich, T. R.; Tominaga, T. *J. Phys. Chem. Ref. Data* **1983**, *12*, 163−178.
(71) Mochida, I.; Tsuji, K.; Suetsugu, K.; Fujitsui, H.; Takeshita, K. *J. Phys. Chem.* **1980**, *84*, 3159−3162.
(72) Bai, Y.; Sekita, M.; Schmid, M.; Bischof, T.; Steinruumlck, H. P.; Gottfried, J. M. *Phys. Chem. Chem. Phys.* **2010**, *12*, 4336−4344.
(73) Bai, Y.; Buchner, F.; Kellner, J.; Schmid, M.; Vollnhals, F.; Steinruumlck, H. P.; Marbach, H.; Gottfried, J. M. *New. J. Phys.* **2009**, *11*, 125004−125019.
(74) Lukasczyk, T.; Flechtner, K.; Merte, L. R.; Jux, N.; Maier, F.; Gottfried, J. M.; Steinruck, H. P. *J. Phys. Chem. C* **2007**, *111*, 3090−3098.
(75) Hieringer, W.; Flechtner, K.; Kretschmann, A.; Seufert, K.; Auwarter, W.; Barth, J. V.; Gorling, A.; Steinruck, H. P.; Gottfried, J. M. *J. Am. Chem. Soc.* **2011**, *133*, 6206−6222.